arXiv:cond-mat/0310715v2 [cond-mat.mes-hall] 15 Feb 2004

Vortex nucleation through edge states in finite Bose-Einstein condensates

Eric Akkermans and Sankalpa Ghosh

Physics Department, Technion I.I.T. Haifa-32000, Israel

(Dated: March 22, 2022)

Abstract

We study the vortex nucleation in a finite Bose-Einstein condensate. Using a set of non-local and chiral boundary conditions to solve the Schrödinger equation of non-interacting bosons in a rotating trap, we obtain a quantitative expression for the characteristic angular velocity for vortex nucleation in a condensate which is found to be 35% of the transverse harmonic trapping frequency.

PACS numbers: 03.75.Lm, 67.40.-w, 71.70.Di

I. INTRODUCTION

A prominent feature of a superfluid is the way it behaves under rotation [1]. In contrast to a normal fluid, that rotates like a rigid body at thermal equilibrium, the thermodynamically stable state of a superfluid at low enough frequency does not rotate. At higher frequencies, a finite amount of angular momentum appears in the form of vortex filaments at which the superfluid density vanishes. The circulation of the velocity field flow evaluated on a closed contour that encircles the vortex is quantized [2, 3]. This is a consequence of the existence of a macroscopic wavefunction, whose phase changes by an integer multiple of 2π around the vortex filaments. Atomic Bose-Einstein condensates (BEC) [4, 5] provide a reference system where the superfluid behaviour can be studied in the weak-coupling regime.

A set of recent experiments has demonstrated [6, 7, 8, 9, 10, 11, 12, 13, 14] the existence of vortices in atomic condensates. The rotational frequency at which the first vortex is nucleated has been shown to depend on parameters such as the trap geometry (aspect ratio), the nature and the characteristic time of the stirring beam, the number of atoms in the trap and may therefore vary from one experiment to another. The ratio of this characteristic rotational frequency to the transverse harmonic trapping frequency varies in these experiments from 0.1 [12] to 0.7[9].

Most of theoretical studies of vortex nucleation in atomic BEC which preceded these experiments [15, 16, 17, 18, 19, 20], determine the characteristic nucleation frequency of the first vortex from the criterion that the vortex-state becomes the minimum of the thermodynamic free energy of the system evaluated in the co-rotating frame. In [21] the global as well as local stability of the vortex state is discussed within the framework of the Bogoliubov theory [3]. Using the Thomas-Fermi approximation, the thermodynamic characteristic frequency can be expressed [16, 17] in terms of the other system parameters. These works have been reviewed in [22]. The characteristic rotational frequency of the vortex nucleation thus obtained is generally lower than the values observed experimentally [7, 8, 12].

The presence of a vortex in a static condensate is associated with an extra energy relative to the vortex free state. Using the Thomas-Fermi approximation it can be shown that this energy is the highest when the vortex is located at the center of the trap and decreases monotonically as a function of the distance between the center of the vortex and the center of the trap [22, 23, 24]. Within Thomas-Fermi approximation (without any boundary correction)

it can be shown that this energy vanishes at the boundary of the system. Thus we can define the energy of a vortex-state E_v as a function of the distance d, namely the separation between the vortex and the center of the trap and $E_v(d)$ has a maximum at $d = 0$. For an increasing rotational frequency this maximum is shifted from the center to the boundary of the system [22, 23] and at rotational frequencies higher than the thermodynamic characteristic frequency this leads to a surface energy barrier to the nucleation of a vortex. This explains why a vortex cannot be nucleated in a trapped condensate even though the trap is rotated at the thermodynamic characteristic frequency. The characteristic frequency for the vortex nucleation can be determined if one knows under what condition and at what rotational frequency a state carrying finite angular momentum will be transferred from the surface to the bulk of the condensate by overcoming the surface energy barrier. Theoretical studies in this direction have been done in [23, 25, 26, 27, 28, 29, 30, 31, 32]. They are based on an analysis of the collective excitations localized at the surface of the condensate, namely the surface modes [33]. These modes appear as shape deformations that carry a finite angular momentum about the axis of rotation [28] and have no radial node. In a rotated condensate these surface modes are excited and this leads to the vortex nucleation. A generalization of the Landau criterion [4, 28, 34] allows to determine at what rotational frequency, the surface mode corresponding to a given angular momentum quantum number is excited and leads to the nucleation of a vortex. The characteristic nucleation determined in this way agrees with the value experimentally observed [30]. Vortices are also nucleated by exciting a particular surface mode through a controlled trap deformation [9, 14] and this problem has been theoretically studied in [23, 29].

Thus far theoretical studies of the problem of vortex nucleation in a trapped condensate has been conducted in the framework of interacting bosons using various approximation schemes. It is also known that the stable state of a set of non-interacting bosons in an axisymmetric harmonic trap does not have finite angular momentum along the z-direction for a rotational frequency less than the trap frequency. A finite amount of interaction makes vortex states energetically feasible at a lower rotational frequency. In this article we study the nucleation of a vortex from the surface to the bulk of a system by solving the one-particle Schrödinger equation with a set of non-local and chiral boundary conditions. To that purpose we start by discussing in section II the role of boundary conditions in a many-body problem. In section III, we review the problem of a trapped boson rotating at a given

frequency in an infinite plane and briefly discuss the corresponding energy spectrum in a finite disc while applying Dirichlet boundary conditions. In section (IV) we introduce the chiral boundary conditions for rotating bosons in a disc and we show how the Hilbert space splits into bulk and edge states. We subsequently analyze the nucleation mechanism, *i.e.* the transfer of angular momentum form edge to bulk. The characteristic angular rotation is given in terms of the trap frequency at which the first and then successive vortices are nucleated in the bulk. The variation of the size of the bulk region with increasing rotation is discussed and its physical implication is pointed out.

II. ROLE OF THE BOUNDARY CONDITIONS IN A MANY BODY PROBLEM

We start with the following hamiltonian corresponding to N interacting bosons of mass m

$$H_{mb} = \sum_{i=1}^{N} -\frac{\hbar^2}{2m}\nabla_i^2 + \sum_{i,j} V(|\boldsymbol{r}_i - \boldsymbol{r}_j|) - E_0 \tag{1}$$

where E_0 is the ground state energy. Except for some specific cases, one does not know how to diagonalize this hamiltonian. Therefore some approximation schemes must be defined whose purpose is to obtain an effective quadratic hamiltonian. We may consider, for instance, the Feynman description [35] that accounts for the excited states under the form

$$\phi(\boldsymbol{r}_1, \cdots, \boldsymbol{r}_N) = F\phi_0(\boldsymbol{r}_1, \cdots, \boldsymbol{r}_N) \tag{2}$$

where ϕ_0 is the exact but unknown ground state wavefunction such that $H_{mb}\phi_0 = 0$, and we assume that $F = \sum_i^N f(\boldsymbol{r}_i)$. The writing of F as a sum over one body terms is exact for the non-interacting problem. For the interacting case, such a decomposition assumes that the interaction is adiabatically switched on. The wavefunction $\phi(\boldsymbol{r})$ is obtained by minimizing the energy

$$E = \frac{\int \phi^* H_{mb}\phi d^N\boldsymbol{r}}{\int |\phi|^2 d^N\boldsymbol{r}} \tag{3}$$

where $d^N\boldsymbol{r} = d\boldsymbol{r}_1 \cdots d\boldsymbol{r}_N$. It can be shown that [35, 36] the effective energy E can be written as

$$E = -\rho_0 \frac{\hbar^2}{2m} \int d\boldsymbol{r} f^*(\boldsymbol{r})\nabla^2 f(\boldsymbol{r}) \tag{4}$$

where ρ_0 is the ground state density. To obtain the corresponding spectrum, we have to impose boundary conditions on $f(\boldsymbol{r})$. Assuming translational invariance, Feynman obtained

that $E = \frac{\hbar^2}{2m}[\frac{k^2}{S(k)}]$, where $S(k)$ is the structure factor. In a trapped condensate the translational invariance is broken by the presence of a confinement potential. The function $f(\boldsymbol{r})$ is related to the order parameter $\Psi(\boldsymbol{r})$. The choices for boundary conditions on the order parameter $\Psi(\boldsymbol{r})$ is broad as it depends on the nature of the confining potential and on the effective one body term generated by the interaction. It might be thus possible to take into account at least partly the effect of interactions by solving a linear Schrödinger like equation under suitable choices of boundary conditions. However in the absence of a specific relation between such boundary conditions and the effective interactions, these choices are generally guided by the nature of the problem.

In this paper we study the vortex nucleation in a confined geometry by solving a one-particle Schrödinger equation for the condensate wavefunction $\Psi(\boldsymbol{r})$ with a set of non-local and chiral boundary conditions. Such boundary conditions have been proposed in order to deal with such non-linear problems [37]. These boundary conditions are motivated by the following considerations. We know [23, 25, 26, 27, 28, 29, 30, 31, 32] that the dispersion relation for the surface excitations determines the characteristic rotational frequency of vortex nucleation. The proposed boundary conditions are designed in order to provide a clear distinction between the bulk and edge states of a two dimensional rotating boson gas. The angular momentum quantum numbers of edge states as we shall see are higher than those of bulk states. Vortices are then nucleated by transferring a state from the edge to the bulk Hilbert spaces.

III. A ROTATING TWO DIMENSIONAL BOSON GAS

A. Hamiltonian and energy spectrum for the infinite plane

We consider the hamiltonian of a trapped boson in a two dimensional domain rotating with a uniform angular frequency Ω :

$$H = \frac{\mathbf{p}^2}{2m} + \frac{1}{2}m\omega^2 r^2 - \Omega L_z \tag{5}$$

We define the vector potential

$$\mathbf{A}_f = \boldsymbol{f} \times \mathbf{r} \tag{6}$$

where $\boldsymbol{f} = (0, 0, f)$. Corresponding pseudo-magnetic fields may be defined by

$$\mathbf{B}_f = \boldsymbol{\nabla} \times \mathbf{A}_f = 2\boldsymbol{f} \tag{7}$$

where f is either ω or Ω so that the hamiltonian (5) rewrites under the two equivalent forms

$$H = \frac{1}{2m}(\mathbf{p} - m\mathbf{A}_\omega)^2 + (\omega - \Omega)L_z \tag{8}$$

or

$$H = \frac{1}{2m}(\mathbf{p} - m\mathbf{A}_\Omega)^2 + \frac{1}{2}m(\omega^2 - \Omega^2)r^2 \tag{9}$$

For $\omega = \Omega$, this hamiltonian is the Landau hamiltonian of a charged particle in a transverse magnetic field written in the symmetric gauge. For this special value the centrifugal force just offsets the confinement and hence the bosonic system becomes unstable.

The eigenfunctions $\Psi_{n,l}$ and the eigenvalues $E_{n,l}$ of the hamiltonian for the infinite plane are characterized by two integer quantum numbers n, l where $n \in \mathbf{N}, l \in \mathbf{Z}$. We define $b_\omega = \frac{m\omega}{\hbar}$ and $b_\Omega = \frac{m\Omega}{\hbar}$. The solutions of the corresponding Schrödinger equation are

$$\Psi_{n,l}(r) = C_{n,l} r^{|l|} e^{il\theta} e^{-\frac{b_\omega r^2}{2}} \; {}_1F_1(a, |l| + 1; b_\omega r^2) \tag{10}$$

where $a = \frac{|l| - \frac{\Omega}{\omega} l + 1}{2} - \frac{e}{4} = -n$ with $e = \frac{2E_{n,l}}{\hbar\omega}$. ${}_1F_1(a, c; x)$ is the confluent hypergeometric function [38, 39] and $C_{n,l}$ is a normalization constant. The eigenenergies are

$$E_{n,l} = \hbar\omega(2n + |l| - \frac{\Omega}{\omega} l + 1) \tag{11}$$

For $l < 0$, the eigenvalues increase with increasing Ω, whereas for $l > 0$, they decrease with increasing Ω. For $\frac{\Omega}{\omega} < 1$, the ground state is always characterized by $n = 0, l = 0$ so that no vortex is nucleated. For $\Omega = \omega$, the energy spectrum is made of Landau levels that are degenerate in angular momentum.

The current density in a given eigenstate is defined by

$$\mathbf{j} = \frac{\hbar}{2mi}(\Psi^*_{n,l} \boldsymbol{\nabla} \Psi_{n,l} - \Psi_{n,l} \boldsymbol{\nabla} \Psi^*_{n,l} - 2i\frac{m}{\hbar} \mathbf{A}_\mathbf{\Omega} |\Psi_{n,l}|^2) \tag{12}$$

Its radial component vanishes while its azimuthal component is

$$j_\theta = \frac{\hbar}{m}(\frac{l}{r} - \frac{m}{\hbar}\Omega r)|\Psi_{n,l}|^2 \tag{13}$$

We define the angular momentum dependent radius r_l by

$$r_l = \sqrt{\frac{l}{b_\Omega}} \tag{14}$$

For a given angular momentum state, $j_\theta(r)$ is positive for $r < r_l$ and hence it gives a paramagnetic contribution. It is negative and diamagnetic for $r > r_l$ and it vanishes at $r = r_l$.

B. Spectrum with Dirichlet boundary conditions (DBC)

We consider now the problem of a trapped rotating boson in a disc of radius R imposing Dirichlet boundary conditions. The corresponding spectrum is derived in the same way as for the electron in a perpendicular magnetic field [36, 40, 41, 42].

The Dirichlet boundary condition (DBC) $\Psi_{n,l}(r = R) = 0$, is according to (10) ${}_1F_1(a, |l|+1; \Phi) = 0$ where $\Phi = b_\omega R^2$ is equivalent to the magnetic flux. The energy spectrum is obtained from the zeroes of the confluent hypergeometric function ${}_1F_1$, that can be separated into two classes according to the sign of the corresponding angular momentum. For $l \geq 0$, the energy levels are given by

$$ {}_1F_1\big(\frac{l(1-\frac{\Omega}{\omega})+1}{2} - \frac{\varepsilon}{4\Phi}, l+1; \Phi\big) = 0 \tag{15}$$

with $\varepsilon = \frac{2mE_{n,l}R^2}{\hbar^2} = e\Phi$. For $l < 0$ the energy levels are given by

$$ {}_1F_1(\frac{-l(1+\frac{\Omega}{\omega})+1}{2} - \frac{\varepsilon}{4\Phi}, -l+1; \Phi) = 0 \tag{16}$$

It is important to notice that the equation ${}_1F_1(a, c; x) = 0$ has solutions only for $a < 0$ and, in the interval $-p < a < -p+1$, it has exactly p real solutions. This eliminates the possibility of having for rotating bosons, a ground state given by the lowest Landau level solution for which $\frac{\varepsilon}{4\Phi} = \frac{l(1-\frac{\Omega}{\omega})+1}{2}$.

The infinite plane solutions are reached asymptotically for large $\frac{\Omega}{\omega}$ (see Fig.1). There is no difference in this spectrum between bulk and edge states. For $\frac{\Omega}{\omega} < 1$, the state $(n, l) = (0, 0)$ is always the ground state (Fig.1). The energy levels become degenerate in angular momentum when $\frac{\Omega}{\omega} = 1$ and $\Phi \gg 1$ (Fig. 2 and [36]). Therefore at zero temperature, no vortex can be nucleated at $\frac{\Omega}{\omega} < 1$ under the DBC.

We have plotted the energy as a function of the angular momentum for a fixed Φ in Fig. 3. For the Landau problem of a charged particle in a transverse magnetic field a similar plot, but in a different geometry and only for positive angular momentum states, has been used in [43] in order to describe the role of the edge states in the quantum Hall transport. In

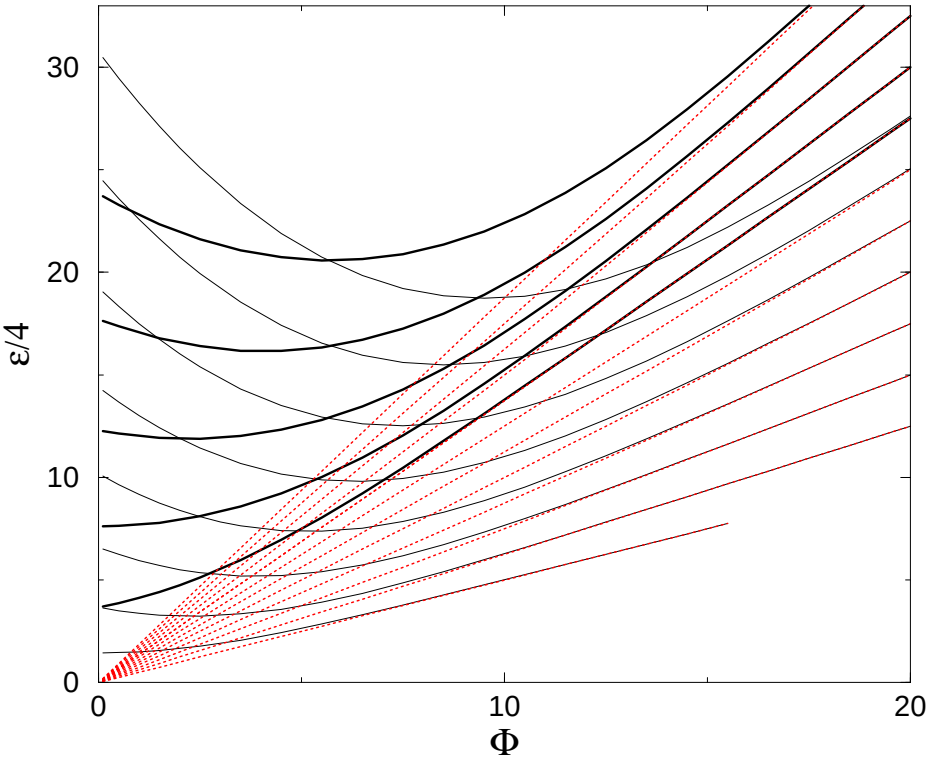


FIG. 1: *Energy spectrum of rotating bosons with Dirichlet boundary condition. The continuous lines (thin lines for* $n = 0$ *and thick lines for* $n = 1$*) correspond to the energy spectrum derived from (15). Each curve corresponds to a given value of the angular momentum. They correspond to* $n = 0$ *and* $l = 0, 1, 2, 3, 4, 5, 6, 7$ *as well as* $n = 1$ *and* $l = -1, 0, 1, 2, 3$*. The dotted lines represent the corresponding infinite plane solutions given by (11). Here* Ω *is taken to be* $.75\omega$*.*

the present problem as well as in the Landau problem there is no sharp difference between edge and bulk states under DBC.

IV. CHIRAL BOUNDARY CONDITIONS

Dirichlet boundary conditions do not provide a way to separate edge from bulk excitations. As already pointed out, such a separation is necessary for the description of the nucleation of a vortex. We therefore propose a set of non-local and chiral boundary conditions which are more suitable for the present problem. These boundary conditions are

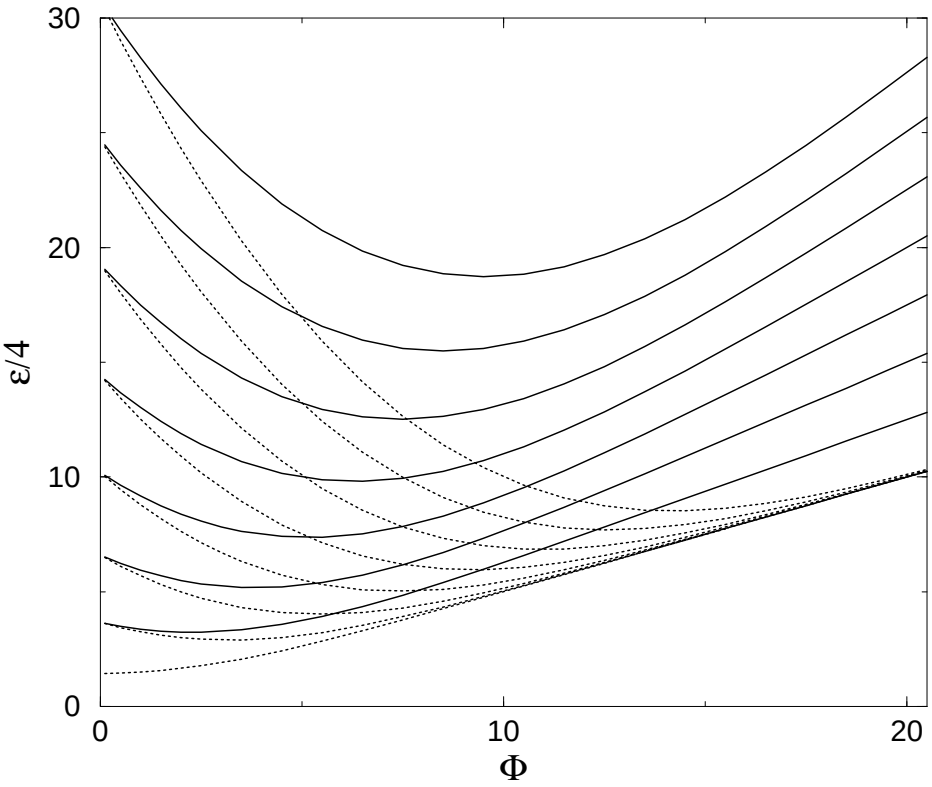


FIG. 2: *Comparison between the energy spectrum of an electron in a transverse magnetic field (dotted lines) and a rotating boson under DBC (continuous lines). The latter is obtained by setting* $\frac{\Omega}{\omega} = 1$ *in (15). For the curves corresponding to the rotating boson* $\frac{\Omega}{\omega}$ *is taken to be* 0.75*. Only the lowest Landau level (*$n = 0$*) is displayed for both cases. We have plotted the energy levels for* l *between* 0 *and* 7*.*

akin to the one introduced by Atiyah, Patodi and Singer (APS) in their study of Index theorems for Dirac operators with boundaries [44]. Similar boundary conditions have also been applied to the Landau problem on manifolds with boundaries [41, 42]. These boundary conditions split the Hilbert space into a direct sum of two orthogonal, *infinite dimensional* spaces with positive and negative chirality on the boundary. The chirality is determined by the direction of the azimuthal velocity projected on the boundary. A vortex is nucleated as a result of the transfer of a state from the edge to the bulk.

We have already noticed that for a given value of the angular momentum l, the current flows with a different chirality in regions separated by a ring of radius $r_l = \sqrt{\frac{l}{\Phi_\Omega}}$. We

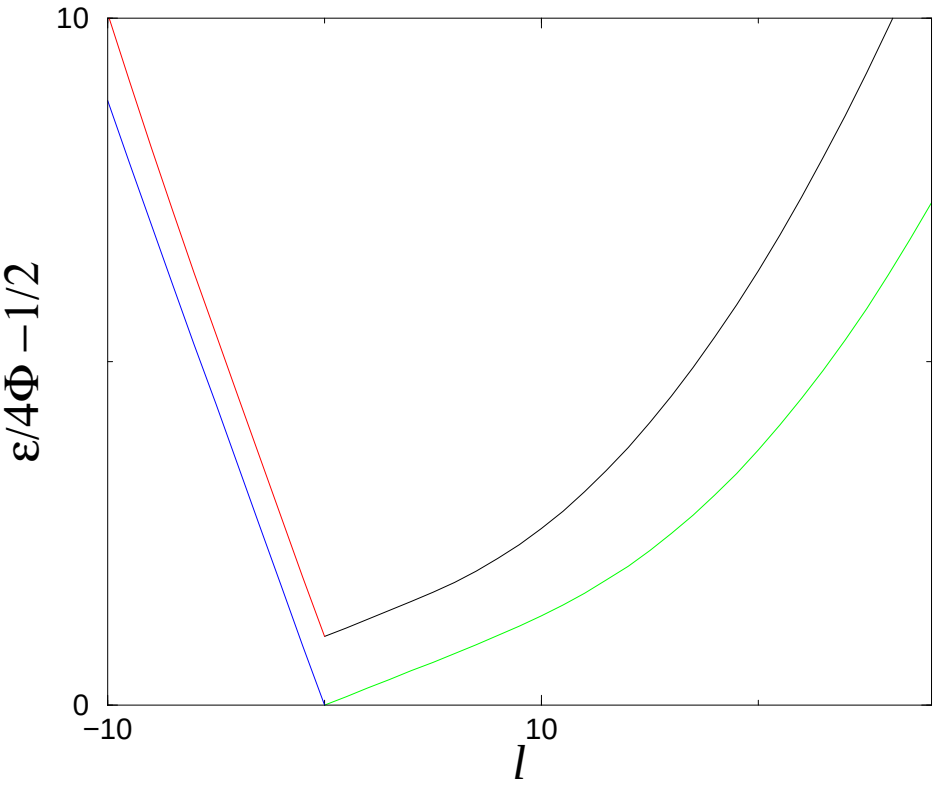


FIG. 3: *Edge and bulk states with DBC. The energy levels that correspond to the first two Landau levels are shown. The lower level corresponds to* $n = 0$ *and the upper one corresponds to* $n = 1$. Φ *and the ratio* $\frac{\Omega}{\omega}$ *are respectively taken to* 20 *and* 0.75.

define the bulk and the edge regions using this particular value of r_l as a reference for a given angular momentum. The current associated to that particular angular momentum is respectively paramagnetic and diamagnetic in the bulk and at the edge. Alternatively, we define the bulk and at the edge states for a disc of size R so that bulk states have angular momentum $l < b_\Omega R^2$ whereas edge states have $l \geq b_\Omega R^2$.

The azimuthal velocity $\frac{j_\theta(r)}{|\psi(\vec{r})|^2}$, projected on the boundary of the disc has eigenvalues given by

$$\lambda(R) = \frac{1}{R}(l - b_\Omega R^2) = \frac{1}{R}(l - \Phi_\Omega) \tag{17}$$

where $\Phi_\Omega = b_\Omega R^2$. The chiral boundary conditions are now defined in the following way:

For $\lambda \geq 0$, namely for $0 < \Phi_\Omega \leq l$

$$\partial_r \psi_l|_R = 0 \tag{18}$$

(For any n and henceforth we shall drop the subscript n in ψ.)

For $\lambda < 0$, namely for $l < \Phi_\Omega$

$$(\frac{\partial}{\partial r} + \frac{i\partial}{r\partial\theta} + b_\Omega r)\Psi_l|_{r=R} = 0 \tag{19}$$

For the first set of wavefunctions that accounts for the edge states we use Neumann boundary conditions. We could have used as well Dirichlet boundary conditions. However unlike Neumann boundary conditions they give an unphysical discontinuity [41]. These wavefunctions are more and more localized towards the outer side of the system for an increasing rotation frequency. For states $l < \Phi_\Omega$, that corresponds to wavefunctions localized well inside the disc, we impose the mixed boundary condition (19). It is this separation in the dispersion relations of the edge states under the choice of CBC that mimics the effect of interactions. In the many-body theory of vortex nucleation this separation is achieved by solving the Bogoliubov equations under various approximations [28, 30, 32] and then by identifying the collective excitations localized at the surface of the condensate.

A. Spectrum with CBC

According to the chiral boundary conditions when Φ is increased at a fixed $\frac{\Omega}{\omega}$, the sign of the eigenvalues $\lambda(R)$ changes from the positive to the negative. Correspondingly the energy ε of a state with a given n and l changes. This change in energy describes how the corresponding state is transferred from the edge Hilbert space to the bulk Hilbert space at the point $\Phi_\Omega = l$ (18). This is shown in Fig.4. For large Φ, the infinite plane solutions (11) are reached asymptotically.

For an infinite system we have $\frac{\varepsilon}{4\Phi} = n + \frac{1}{2}(1 + (1 - \frac{\Omega}{\omega})l)$. Therefore $\frac{\varepsilon}{4\Phi}$, for a given $\frac{\Omega}{\omega}$, is a linear function of l with slope $(1 - \frac{\Omega}{\omega})$. When chiral boundary conditions are applied, this behaviour is approximately obeyed for the bulk states. But for the edge states the energy increases non-linearly with increasing angular momentum. This is shown in Fig.5. This is also the case for Dirichlet boundary conditions (Fig.3). There is however a quantitative difference and moreover the bulk and the edge states are now separated under these chiral

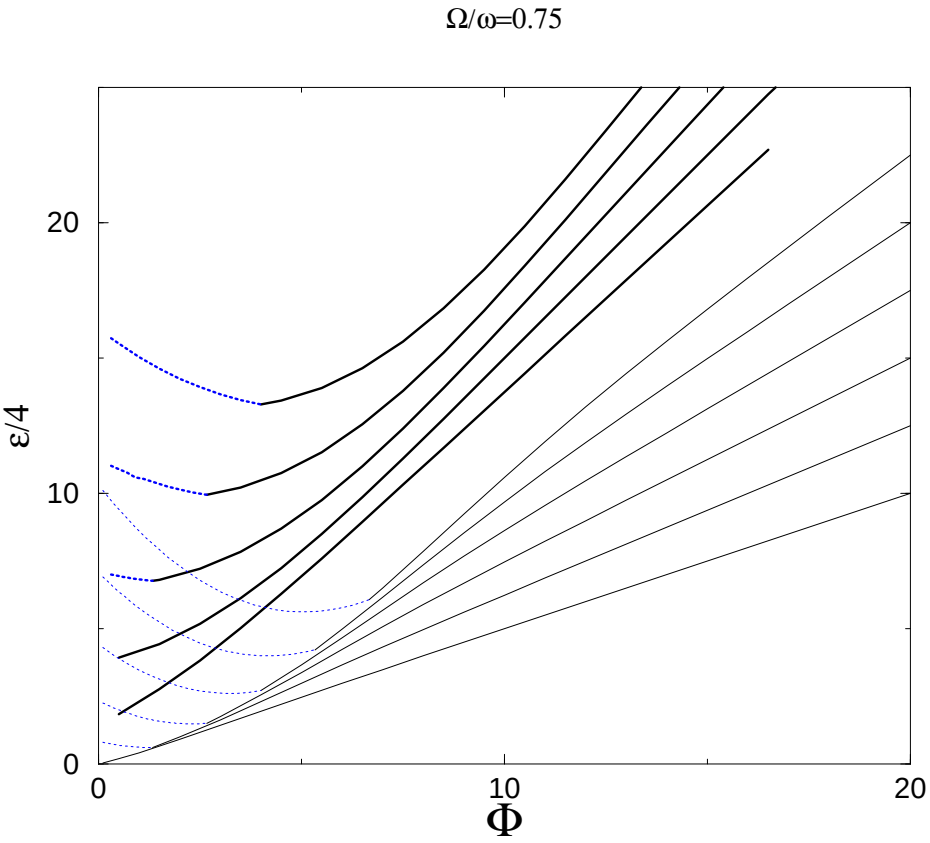


FIG. 4: *Energy levels with chiral boundary condition. Energy levels for the first few angular momentum states are shown for* $n = 0$ *and* $n = 1$*. Each curve corresponds to a given value of the angular momentum. They correspond to* $n = 0$ *and* l *between* 0 *and* 5 *(thin lines for bulk states and thin dotted lines for edge states) as well as* $n = 1$ *and* l *between* -1 *and* 3 *with* $l = -1$ *corresponds to the lowest curve (thick lines for bulk states and thick dotted lines for the edge states). For* $l > 0$ *the spectrum has a kink at the point* $l = \Phi_\Omega = \frac{\Omega}{\omega}\Phi$*.*

boundary conditions. For a given n the spectrum is continuous at the point $l = \Phi_\Omega$, but its derivative is not. This has been shown in Fig.5 for the first two values of n. The derivation of the spectrum under these boundary conditions is provided in detail in the appendix. Here we focus on the nucleation of vortices under these boundary conditions.

The Fig.6 shows the effect of an increase of the rotational frequency on the spectrum under the choice of CBC. We have plotted the energies of the bulk and the edge states

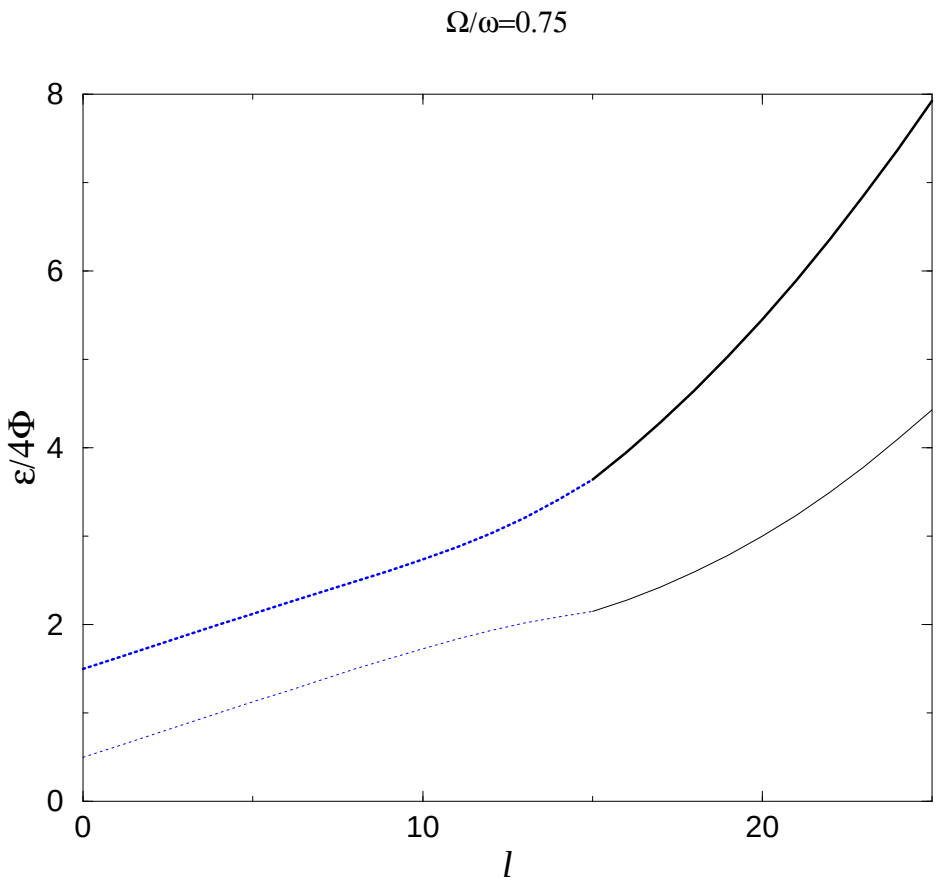


FIG. 5: *Edge and bulk states with chiral boundary conditions. Energy levels that correspond to* $n = 0$*(lower curve) and* $n = 1$ *(upper curve) are shown. Here the edge states are denoted by continuous lines whereas the bulk states are denoted by dotted lines. The slope of the energy levels is discontinuous at* $l = \Phi_\Omega$ *where* Φ_Ω *is taken to be 15.*

for four different values of the ratio $\frac{\Omega}{\omega}$. For each value, the quantity Φ_Ω is increased by unit steps from 1 to 3 and the corresponding bulk and edge energies are shown. Under these conditions, the slope of the bulk energy levels increases while the slope of the edge energy levels goes down. The opposite behaviour is observed when, for a fixed Φ_Ω, the ratio $\frac{\Omega}{\omega}$ increases. Therefore with increasing rotational frequency, states with higher angular momenta are transferred from the edge Hilbert space to the bulk Hilbert space. The l-th angular momentum state is nucleated in the bulk from the edge by changing Φ_Ω from l to $l + 1$.

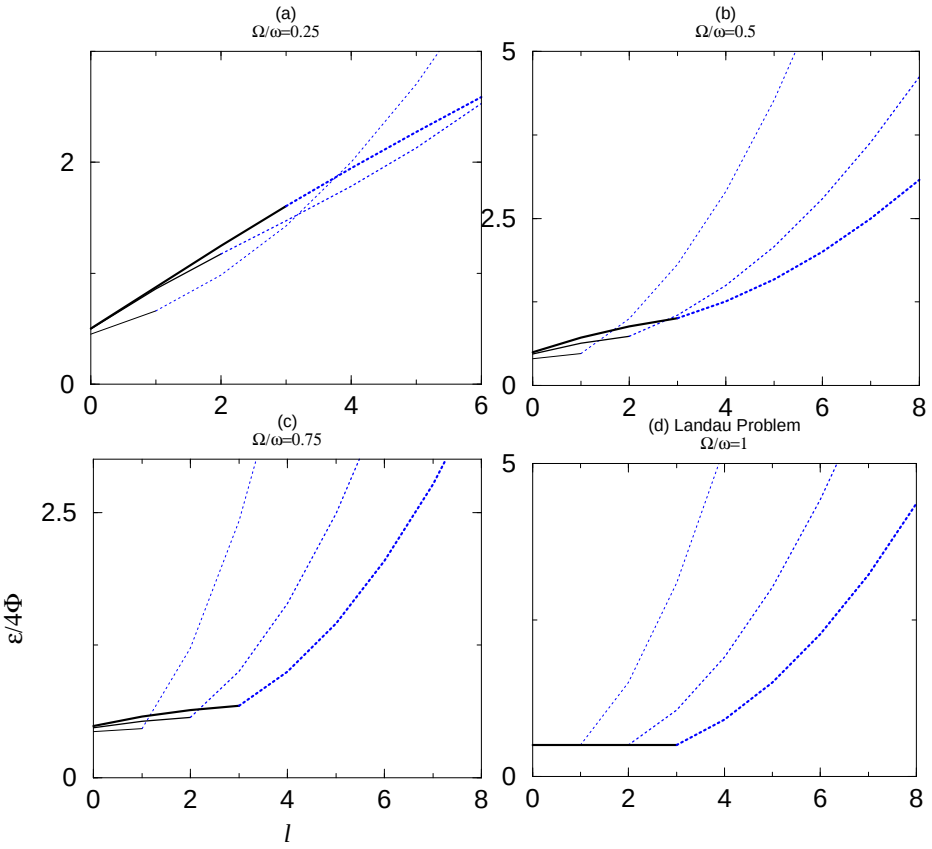


FIG. 6: *Effect of a faster rotation. In these figures we have plotted the energies* $\frac{\varepsilon}{4\Phi}$ *as a function of* l *for a set of* $\frac{\Omega}{\omega}$ *values (given above each figure). The three plots in each figure correspond to* $\Phi_\Omega = 1, 2, 3$ *(the thinnest one for* $\Phi_\Omega = 1$ *and the thickest for* $\Phi_\Omega = 3$*). The dotted part corresponds to edge states while the continuous part corresponds to bulk states. For* $\frac{\Omega}{\omega} = 1$ *bulk states for all three values of* Φ_Ω *fall on the same line.*

The plots that appear in Fig.6 represent solutions of the stationary Schrödinger equation under the choice of CBC at different values of Ω and Φ_Ω. To understand the nucleation of vortices in the condensate with these solutions we use the fact that a condensate is rotated only by nucleating a vortex. Therefore in between nucleations of successive vortices, the radius of the condensate remains constant. This is in contrast to the rotation of a rigid body which flattens out continuously while increasing the rotational frequency. Let us denote by Ω_1, the characteristic frequency for nucleation of the first vortex. For a given $\Omega < \Omega_1$, the radius of the condensate is R and it corresponds to $\Phi_\Omega = 1$. The corresponding

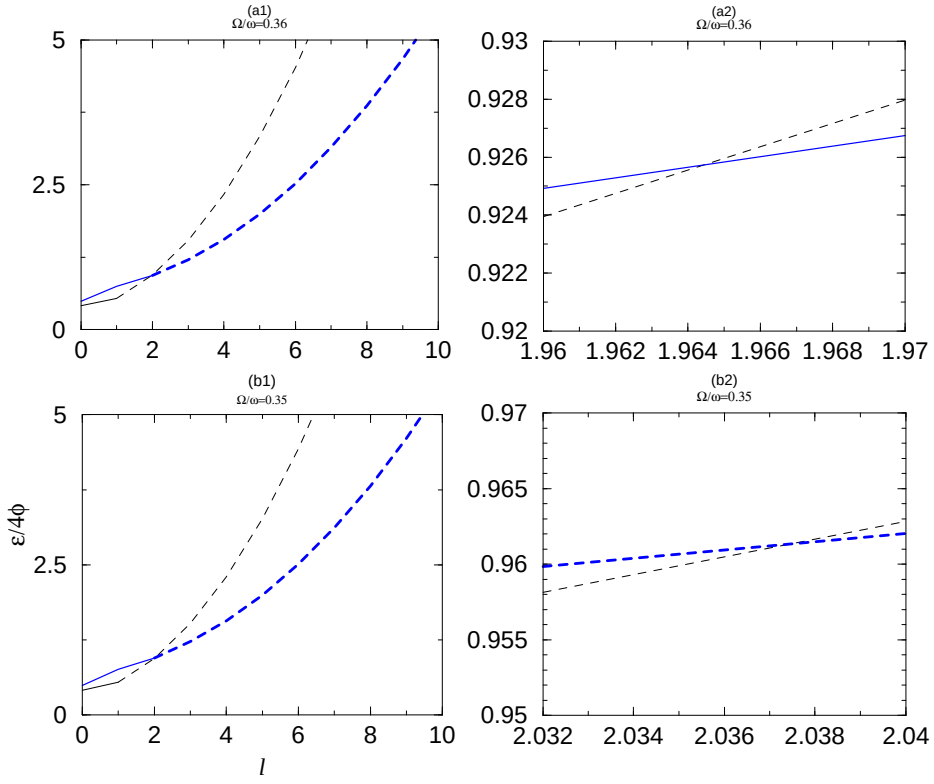


FIG. 7: *Determination of the characteristic frequency of vortex nucleation. In these figures we have plotted the energy* $\frac{\varepsilon}{4\Phi}$ *against the angular momentum* l*. The two curves in each figure correspond to* $\Phi_\Omega = 1$ *(thin),* $\Phi_\Omega = 2$*(thick). Corresponding ratios* $\frac{\Omega}{\omega}$ *are mentioned above each figure. In each curve the continuous part corresponds to bulk states and the dashed-line part to edge states. At* $\frac{\Omega}{\omega} = 0.35$ *the edge spectrum for* $\Phi_\Omega = 1$ *intersects the corresponding edge spectrum for* $\Phi_\Omega = 2$ *(*$b1$ *and* $b2$*). At* $\frac{\Omega}{\omega} = 0.36$*, the intersection takes place between the bulk spectrum for* $\Phi_\Omega = 2$ *and the edge spectrum for* $\Phi_\Omega = 1$ *(*$a1$ *and* $a2$*). The regions near points of intersection are enlarged in the figures* $a2$ *and* $b2$*.*

bulk and edge energy levels for $\Phi_\Omega = 1$ are obtained from (18) and (19). The condensate is therefore the bulk region that contains only the $l = 0$ state. At $\Omega = \Omega_1$, the first vortex is nucleated by transferring the $l = 1$ state from the edge to the bulk so that Φ_Ω changes from 1 to 2. Therefore the condensate is now defined as the bulk region of $\Phi_\Omega = 2$ and it has a larger radius. The rotational flux transferred by nucleating a vortex is thus $\frac{h}{m}$ since this is the unit of Φ_Ω. At $\Omega = \Omega_1$, the edge states for $\Phi_\Omega = 1$ intersects the bulk states for

$\Phi_\Omega = 2$. This is energetically favoured since at $\Omega = \Omega_1$, the energy $\frac{\varepsilon}{4\Phi}(l)$ of any state with $l \geq 2$ is less if $\Phi_\Omega = 2$ rather than $\Phi_\Omega = 1$. In the corresponding many body description [23, 30, 32], vortices are nucleated when at higher rotational frequency, a surface energy barrier disappears. The reduction of the edge state energy with the nucleation of a vortex is qualitatively similar to the disappearance of the surface energy barrier.

The characteristic rotational frequency for the nucleation of the first vortex determined using chiral boundary conditions (18,19) is between $\Omega = 0.35\ \omega$ and $0.36\ \omega$ as shown in Fig.7 where ω is the transverse trap frequency. We note that this characteristic nucleation frequency is close to the value $\Omega = 0.29\ \omega$ that has been observed in one of the experiments on vortex nucleation [11]. All these features cannot be derived from either the infinite plane or from DBC.

To establish a parallel with the case of superconductors let us mention similar results obtained for the vortex nucleation in a mesoscopic superconducting disc [45, 46, 47]. However in a neutral superfluid there is no Maxwell-Ampère equation that can relate the current to the induced rotation .

V. VORTEX NUCLEATION FOR $\Omega > \Omega_1$

Thus far we have discussed the nucleation of the first vortex. Here we discuss the bulk and edge spectrum under CBC for $\Omega > \Omega_1$. We consider the following two cases:

1. For a further increase of Ω beyond Ω_1, the edge states corresponding to $\Phi_\Omega = l$ crosses the bulk states of $\Phi_\Omega = l+1$ for $l \geq 2$ (Fig.6). The corresponding rotational frequencies Ω_l are the nucleation frequencies of the l-th vortices. Each of these vortices is nucleated by changing Φ_Ω to $\Phi_\Omega + 1$ and it carries one unit of angular momentum. Characteristic rotational frequencies are presented in the Table I. Since the bulk and edge energy spectra under CBC is obtained by solving the stationary Schrödinger equation in a co-rotating frame, solutions at different values of Ω can be related one to the other if the rotation is switched on adiabatically. Such experiments [9, 14] have been performed in a deformed rotating trap where the cross-section of the rotating condensate is an ellipse in the plane of rotation. Here we solve the Schrödinger equation in a circular domain. This makes the comparison with the experimental results rather difficult. The theoretical work [29] used an approach different from ours, to explain the nucleation

Vortex	$\frac{\Omega}{\omega}$
1st	0.35 - 0.36
2nd	0.46-0.47
3rd	0.52-0.53
4th	0.569-0.57
5th	$0.603 - 0.604$
6th	$0.629 - 0.630$

TABLE I: *Nucleation frequencies of successive ($l = 1$) vortices.*

mechanism of the first vortex. It should also be noticed that the adiabatic nucleation of successive vortices has not yet been observed experimentally. For a recent theoretical work on this issue see [48]. One of the limitations of our theoretical frame-work is that we are unable to determine the spatial arrangement of more than one vortex inside the condensate.

2. Another interesting point is to find the rotational frequencies at which edge states of $\Phi_\Omega = 1$ intersects the bulk state $l = 2$ for $\Phi_\Omega = 3, 4, \cdots$. The bulk and edge energy levels of the stationary Schrödinger equations at these rotational frequencies correspond to a situation where the rotation is suddenly switched on at a frequency higher than Ω_1 and subsequently the system is brought to equilibrium in the co-rotating frame. More than one angular momentum states (and rotational fluxes) are transferred to the bulk at these characteristic frequencies. This leads to the nucleation of a vortex of angular momentum $l > 1$ or multiple $l = 1$ vortices at a time. Within the present theoretical framework it is not possible to identify which of these two alternatives is energetically favourable. In Table II we have listed these rotational frequencies and the number of angular momenta transferred to the bulk Hilbert space. Around $\frac{\Omega}{\omega} = 0.5$, the number of vortices nucleated in this way increases very fast. Experimentally [10, 11] it has been observed that under sudden switch-on of the rotation at higher rotational frequencies more than one vortices are nucleated and the number of nucleated vortices is the largest, (see for example Fig. 3 in [11]) at $\Omega = \frac{\omega}{\sqrt{2}}$. This is associated with a resonant quadrupolar excitation of angular momentum $l = 2$. The energy of this quadrupolar surface mode in units of the transverse trap frequency is determined

No. of states transferred to the bulk	$\frac{\Omega}{\omega}$
2 $(1,2)$	0.44 - 0.45
3 $(1,2,3)$	0.48-0.49
4 $(1,2,3,4)$	0.494-0.495
5 $(1,2,3,4,5)$	0.498-0.499

TABLE II: *Nucleation frequencies of multiple vortices. In parentheses we mention the angular momentum states which are transferred from the edge to the bulk at these values of* Ω.

within the classical hydrodynamic approximation that is very different from our approach. Therefore although our findings qualitatively agree with these experimental observations, a quantitative comparison with both the experiments and the related theory is rather involved. A reason for that is the difference in the trap geometry in the two-dimensional plane which is elliptical in the experiment while circular in our case. Another reason is the different theoretical approach that have been used to study the surface excitations in the many-body theory [27, 28, 30] and our. The difference between the characteristic rotational frequencies in the above two cases (Table I and II) thus shows that the nucleation frequency of a vortex in the condensate depends on the number of vortices already present.

The radius of the condensate is changed when a vortex is nucleated. Since a boson in the condensate has one more unit of angular momentum when a vortex is nucleated, its orbit has a larger radius. This explains why size of the condensate region increases with successive nucleations. When the l-th vortex with one unit of angular momentum is nucleated, the condensate region corresponds to $\Phi_\Omega = l + 1$. Therefore at each Ω_l, the radius of the condensate region is defined as

$$r_c|_{\Omega=\Omega_l} = \sqrt{\frac{\hbar(l+1)}{m\Omega_l}} \tag{20}$$

Between the nucleations of the l-th and $(l+1)$-th vortex, the radius of the bulk region for $\Phi_\Omega = l$ decreases as $r = \sqrt{\frac{\hbar(l+1)}{m\Omega}}$ and the corresponding edge region grows in size. In Fig.8 using the set of frequencies listed in Table I we have plotted the condensate radius. In

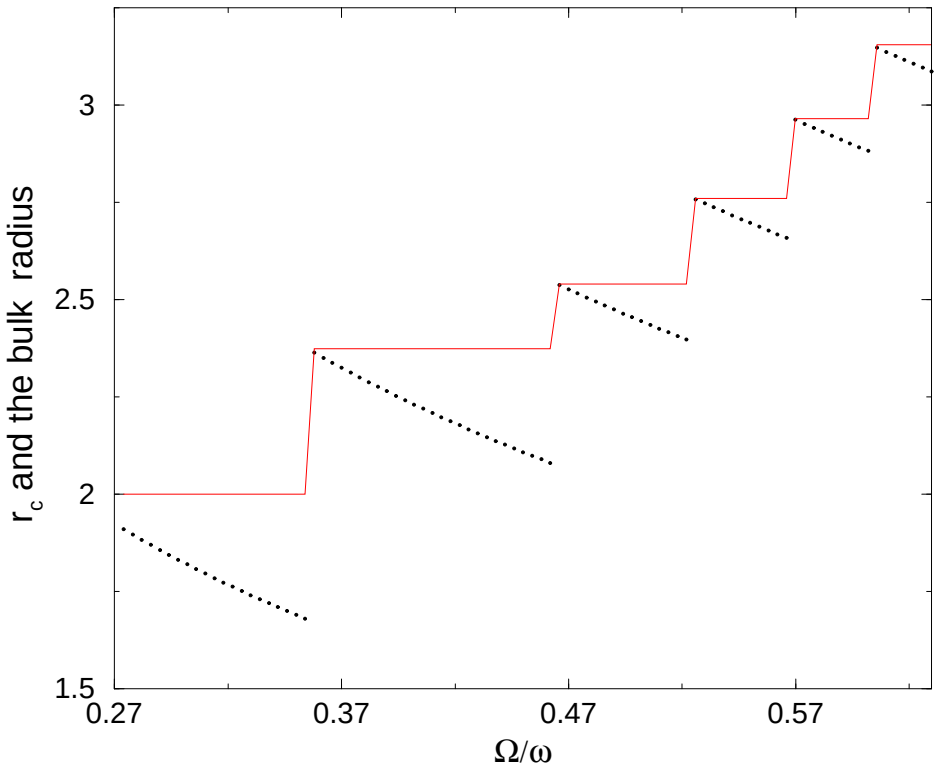


FIG. 8: *Size of the condensate as a function of the rotational frequency. The continuous lines gives the radius of the condensate* r_c *as a function of* $\frac{\Omega}{\omega}$*. The dots give the radius of the bulk region for* $\Phi_\Omega = l$ *and for* $\Omega_l < \Omega < \Omega_{l-1}$*. The length is measured in units of* $\frac{1}{\sqrt{b_\omega}}$ *where* $b_\omega = \frac{m\omega}{\hbar}$.

the same figure we have simultaneously plotted the radius of the bulk region for $\Phi_\Omega = l$, in between the nucleation of the l-th and $(l-1)$-th vortices. This plot involves a set of disconnected lines and the corresponding differences with the condensate region show how the edge region grows between the nucleation of two successive vortices. With the increase of the number of vortices in the condensate these two plots get closer one to the other. In the limit of a large number of vortices, the average rotation approaches the rigid body value [2, 10, 22]. For example, it has been shown in [10] that experimentally this happens when the number of vortices is around 10 [10].

Khawaja *et. al.* [27] have studied the surface excitations of a trapped three-dimensional Bose-Einstein condensed gas using the Gross-Pitaevskii equation and they have associated the kinetic energy of the surface region to an effective surface tension. Although our approach

is different and that we consider a strictly two dimensional system, we can also define an energy associated to the edge by summing the energies of the edge states for $\Phi_\Omega = l$. For a finite system then a part of this edge energy is used to nucleate vortices .

VI. CONCLUSION

We have presented a one-particle effective theory that describes the process of vortex nucleation in a two dimensional rotating condensate using a set of non local and chiral boundary conditions. We have shown that the edge states have a dispersion relation distinct from the bulk states. These boundary conditions can be understood as a way to mimic the effect of the interaction between the bosons. We have demonstrated that the properties of vortices thus nucleated agree qualitatively and quantitatively with experimental findings although a more thorough comparison is not possible in the absence of a precise mapping between this set of boundary conditions and the effective interaction. The expression of the characteristic rotational frequency at which vortices are nucleated under adiabatic and sudden switch-on of the rotation is calculated and the change in the condensate size with increasing rotation is also emphasized.

Acknowledgements

We thank the Israel Council for Higher Education for financial support. This work is supported in part by a grant from the Israel Academy of Sciences and the fund for promotion of research at the Technion.

Appendix I

- *Case 1*: For $\lambda \geq 0 \Rightarrow 0 < \Phi_\Omega \leq l$ plugging the explicit form of the wavefunction (10) in equation (18) we get [39]

$$(\frac{l}{\Phi} - 1)_1F_1(a, l+1; \Phi) + \frac{2a}{l+1}\ {}_1F_1(a+1, l+2; \Phi) = 0 \tag{21}$$

- *Case 2*: For $\lambda < 0$ there are two possibilities

- *Case 2a*: For $l < 0$ (negative angular momentum) the spectral boundary condition (19) implies

$$(\frac{\partial}{\partial r} + \frac{i\partial}{r\partial\theta} + b_\Omega r)\Psi_{n,l}|_{r=R} = 0 \tag{22}$$

  Using the explicit form of wavefunction given in (10) we find that this demands

$$2l\ {}_1F_1(a, |l|; \Phi) - \Phi(1 - \frac{\Omega}{\omega})_1F_1(a, |l|+1; \Phi) = 0 \tag{23}$$

- *Case 2b*: The other situation is where $0 \leq l < \Phi_\Omega$. Again using the explicit form of the wavefunction ($l > 0$) it can be found that

$$\frac{2a}{l+1}\ {}_1F_1(a+1, l+2; \Phi) - (1 - \frac{\Omega}{\omega})_1F_1(a, l+1; \Phi) = 0 \tag{24}$$

- It can be seen that the lowest Landau level solution exists only if $\Omega = \omega$. If we set $2b_\omega = b, \omega = \Omega$ where $b = \frac{m\omega_c}{\hbar}$ and ω_c is the cyclotron frequency, all the above results matches with the results obtained for the Landau problem on a finite disk under chiral boundary condition [41]. We solve all these equation with *Mathematica* [49]

To obtain the characteristic frequencies for the nucleation of successive vortices (Table I) we have solved the equation (21) for $\Phi_\Omega = l$ and $\Phi_\Omega = l + 1$ simultaneously. For $l = 1$ the solution yields $0.35\omega < \Omega < .36\omega$ (Fig. 7). The characteristic frequencies listed in Table II are obtained from simultaneously solving equation (21) with $\Phi_\Omega = 1$ and equation (24) with $\Phi_\Omega = 3, 4, 5, \cdots$.

---

[1] A.J. Legget, Physica Fennica **8**, 125, (1973).

[2] R.P. Feynman, Application of Quantum Mechanics to Liquid Helium in *Progress in Low Temperature Physics I*, Edited by C. J. Gorter (North-Holland Publishing Co., Amsterdam, 1955), Chapter 2.

[3] P. Nozieres and D. Pines, *The Theory of Quantum Liquids, Vol II*, (Addition -Wesley Publishing Company, Inc., 1990).

[4] C. Pethick and H. Smith, Cambridge University Press, *Bose-Einstein Condensation in Dilute gases*, (Cambridge University Press, 2002). For a discussion of the *Landau Criterion* see the Chapter 10.

[5] L. Pitaevskii and S. Stringari, *Bose-Einstein Condensation*, (Oxford Science Publication, 2003).

[6] M.R.Mathews, B.P. Anderson, P.C. Haljan, D.S. Hall, C. E. Weiman and E. A. Cornell, Phys. Rev. Lett. **83** , 2498, (1999).

[7] P.C. Haljan, I. Coddington, P. Engels and E.A. Cornell , Phys. Rev. Lett. **87**, 210403, (2001).

[8] K.W.Madison, F. Chevy, V. Bretin and J. Dalibard, Phys. Rev. Lett. **84**, 806, (2000); F. Chevy, K.W.Madison and J. Dalibard, Phys. Rev. Lett. **85**, 2223, (2000).

[9] K.W.Madison, F. Chevy, V. Bretin and J. Dalibard, Phys. Rev. Lett. **86**, 4443, (2001).

[10] F. Chevy, K.W. Madison, V. Bretin and J. Dalibard, arXiv:cond-mat/0104218.

[11] J. R. Abo Shaeer, C. Raman, J.M. Vogels and W. Ketterle, Science **292**, 476, (2001).

[12] C. R. Raman, J. R. Abo-Shaeer, J. M. Vogels, K. Xu and W. Ketterle, Phys. Rev. Lett. **87**, 210402, (2001).

[13] P. Rosenbusch, V. Bretin and J. Dalibard, Phys. Rev. Lett. **89**, 200403, (2002).

[14] E. Hodby, G. Hechenblaikner, S. A. Hopkins, O. M. Maragò, and C. J. Foot, Phys. Rev. Lett. **88**, 010405 (2002).

[15] F. Dalfovo and S. Stringari, Phys. Rev. A **53**, 2477, (1996).

[16] E. Lundh, C. J. Pethick and H. Smith, Phys. Rev. A **55**, 2126, (1997).

[17] S. Sinha, Phys. Rev. A **55**, 4325, (1997).

[18] Y. Castin and R. Dum, Eur. Phys. J. D **7**, 399 (1999).

[19] D. L. Feder, C. W. Clark and B. I. Schneider, Phys. Rev. Lett. **82**, 4956, (1999).

[20] D. A. Butts and D. S. Rokshar, Nature **397**, 327, (1999).

[21] T. Isoshima and K. Machida, Phys. Rev. A, **60**, 3313, (1999).

[22] A. L. Fetter and A. A. Svidzinsky, J. Phys. C **13**, R135, (2001).

[23] M. Kraemer, L. Pitaevskii, S. Stringari and F. Zambelli, Laser Physics **12**(1), 113 (2002).

[24] M. Guilleumas and R. Graham, Phys. Rev. A, **64**, 033607 (2001)

[25] S. Stringari, Phys. Rev. Lett. **77**, 2360, (1996).

[26] A. Recati, F. Zambelli and S. Stringari, Phys. Rev. Lett. **86**, 377, (2001).

[27] U. A. Khawaja, C. J. Pethick, and H. Smith, Phys. Rev. A **60**, 1507, (1999).

[28] F. Dalfovo and S. Stringari, Phys. Rev. A **63**, 011601(R), (2000).

[29] S. Sinha and Y. Castin, Phys. Rev. Lett. **87**, 190402 (2001)

[30] J. R. Anglin, Phys. Rev. Lett. **87**, 240401, (2001), *ibid* Phys. Rev. A **65**, 063611, (2002).

[31] A. E. Muryshev and P. O. Fedichev, cond-mat/0106462.

[32] T. P. Simula, S. M. M. Virtanen and M. M. Saloma, Phys. Rev. A **66**, 035601, (2002).

[33] R. Onofrio, D. S. Durfee, C. Raman, M. Köhl, C. E. Kuklewicz and W. Ketterle, Phys. Rev. Lett. **84**, 810, (2000).

[34] L. D. Landau, J. Phys. (U.S.S.R), **5**, 71, (1941).

[35] R. P. Feynman, Phys. Rev. **94**, 262 (1954).

[36] E. Akkermans and R. Narevich, Phil Mag. B, **77**, 1097 (1998).

[37] E. Akkermans and K. Mallick, in *Topological aspects of low dimensional systems*, Les Houches Summer School, Session **LXIX** (Springer, Berlin 1999); cond-mat/9907441. §3.5 is particularly relevent for the present discussion.

[38] F. G. Tricomi, Fonctions Hypergéometriques Confluentes, Mémorial des Sciences Mathématiques, CXL, (1960).

[39] M. Abramowitz and I. A. Stegun, *Handbook of Mathematical Functions*, (Dover Publications, New York, 1968).

[40] E. Akkermans, J. E. Avron, R. Narevich and R. Seiler, The Eur. Phys. J. B **1**, 117-121, (1998).

[41] E.Akkermans and R. Narevich (*unpublished*).

[42] R. Narevich, *Ph.D.thesis*, Technion I.I.T,Israel (*unpublished*)

[43] B. I. Halperin, Phys. Rev. B. **25**, 2185, (1982.)

[44] M. Atiyah, V. Patodi, I Singer, *Math. Proc. Camb. Phys. Soc.*, **77**, 43, (1975).

[45] A. K. Geim *et. al.*, Nature, **390**, 259 (1997), P. Singh. Deo, V. A. Schweigert, F. M. Peeters, and A. K. Geim, Phys. Rev. Lett., **79**, 4653 (1997).

[46] E. Akkermans and K. Mallick, J. Phys. A **32**, 7133 (1999) and E. Akkermans, D. M. Gangardt and K. Mallik, Phys. Rev. B **62**, 12427, (2000).

[47] C. Bolech, G. C. Buscaglia and A. López, Phys. Rev. B **52**, R15179 (1995).

[48] C. Lobo, A. Sinatra and Y. Castin, Phys. Rev. Lett, **92**, 020403 (2004).

[49] S. Wolfram, *The MATHEMATICA BOOK*, (Cambridge University Press, 1996), Third Edition.